

## ARTICLE OPEN



# NCX1 coupled with TRPC1 to promote gastric cancer via $\text{Ca}^{2+}$ /AKT/ $\beta$ -catenin pathway

Hanxing Wan<sup>1,2,5</sup>, Nannan Gao<sup>1,2,5</sup>, Wei Lu<sup>1</sup>, Cheng Lu<sup>2</sup>, Jun Chen<sup>2</sup>, Yimin Wang<sup>3</sup> and Hui Dong<sup>1,4</sup>✉

© The Author(s) 2022

Plasma membrane  $\text{Na}^+/\text{Ca}^{2+}$  exchanger 1 (NCX1) is a bidirectional ion transporter to operate in  $\text{Ca}^{2+}$  entry or exit modes, and TRPC1 is  $\text{Ca}^{2+}$ -permeable channel. Both NCX1 and TRPC1 play critical roles in maintaining cytosolic free  $\text{Ca}^{2+}$  ( $[\text{Ca}^{2+}]_{\text{cyt}}$ ) homeostasis in mammalian cells. Although either TRPC1 channel or  $\text{Ca}^{2+}$  entry mode of NCX1 is implicated in some tumorigenesis, it has not been explored if a coordination of NCX1 and TRPC1 involves in the pathogenesis of *H. pylori*-associated human gastric cancer (GC). Here we found the protein expression of NCX1 was significantly enhanced in human GC specimens, which correlated with tumor progression and poor survival in GC patients. TRPC1 and NCX1 were parallelly enhanced, co-localized and bound in human GC cells. By a functional coupling, TRPC1 drives NCX1 to the  $\text{Ca}^{2+}$  entry mode, raising  $[\text{Ca}^{2+}]_{\text{cyt}}$  in GC cells. Moreover,  $\text{CaCl}_2$ , *H. pylori* and their virulence factors all enhanced expressions and activities of NCX1 and TRPC1, and evoked aberrant  $\text{Ca}^{2+}$  entry to promote proliferation, migration, and invasion of GC cells through AKT/ $\beta$ -catenin pathway. Tumor growth and metastasis also depended on the enhanced expression of NCX1 in subcutaneously xenografted GC mouse model. Overall, our findings indicate that TRPC1/NCX1 coupling may promote *H. pylori*-associated GC through the  $\text{Ca}^{2+}$ /AKT/ $\beta$ -catenin pathway. Since the  $\text{Ca}^{2+}$  exit mode and the  $\text{Ca}^{2+}$  entry mode of NCX1 play different roles under mostly physiological and pathological conditions respectively, targeting TRPC1/NCX1 coupling could be a novel strategy for selectively blocking  $\text{Ca}^{2+}$  entry mode to potentially treat digestive cancer with less side effect.

Oncogene (2022) 41:4169–4182; <https://doi.org/10.1038/s41388-022-02412-9>

## INTRODUCTION

Since gastric cancer (GC), one of the leading causes of cancer-related death worldwide, is difficult to cure once it metastasizes [1], it is urgent to explore early diagnostic markers and novel therapeutic targets responsible for GC. *Helicobacter pylori* (*Hp*) infection in the stomach is a well-known risk factor for GC and ammonia/ammonium is the major *Hp* virulence factor [2], but their pathogenesis in GC is still obscure. Therefore, it is critical to elucidate molecular pathogenesis of *Hp*-associated GC. Cytosolic free  $\text{Ca}^{2+}$  ( $[\text{Ca}^{2+}]_{\text{cyt}}$ ) is a pivotal second messenger in eukaryotic cells to maintain critical cellular processes, including the energetic metabolism, cell signaling, and cell motility, etc [3–5]. Numerous findings indicate that aberrant  $[\text{Ca}^{2+}]_{\text{cyt}}$  signaling is involved in GC, though the occurrence and progression of cancer are complex [6–8]. Since membrane  $\text{Ca}^{2+}$ -permeable channels and transporters play important roles in the regulation of  $[\text{Ca}^{2+}]_{\text{cyt}}$ , their aberrant expression and function are associated with GC development [9–11].

The  $\text{Na}^+/\text{Ca}^{2+}$  exchanger (NCX) is a bidirectional transporter that induces  $\text{Ca}^{2+}$  efflux (when operating in  $\text{Ca}^{2+}$  exit mode), or  $\text{Ca}^{2+}$  influx (when operating in  $\text{Ca}^{2+}$  entry mode), depending on the electrochemical gradient of the substrate ions and membrane potentials [12]. Three different protein isoforms of NCX were described [12], NCX1 has a broad expression in multiple organs,

including the heart, kidney, and gastrointestinal (GI) tract, etc, whereas NCX2 is mainly found in the brain but NCX3 mostly in brain and skeletal muscle [13, 14]. NCX has been investigated predominately in human brain, heart and kidney, and the therapeutic potentials of its modulators are also emerging for the related disease. However, the molecular and functional aspects of NCX in GI organs, especially in GI cancer are scarce although it is involved in aberrant  $[\text{Ca}^{2+}]_{\text{cyt}}$  homeostasis in other cancer cells [15]. It has been shown that NCX1 is expressed in the rat small intestine [16]. Although the expression and function of NCX were reported in human gastric smooth muscle cells and myofibroblasts [17], they have not been explored in gastric epithelium. Furthermore, emerging evidence suggests a pathogenesis role of NCX in glioblastoma, melanoma, and ovary carcinoma [15]. We and others also revealed a role of NCX1 in esophageal squamous cell carcinoma and hepatocellular carcinoma [18, 19], but its role in the adenocarcinoma of GI tract has not been explored so far.

Transient receptor potential canonical (TRPC) channels as  $\text{Ca}^{2+}$ -permeable channels are ubiquitously expressed in various cell types, including GI epithelial cells to regulate  $[\text{Ca}^{2+}]_{\text{cyt}}$  homeostasis [20]. Among seven members of TRPC subfamilies, TRPC1 is crucial for metastasis by epithelial-mesenchymal transition (EMT) activation in several kinds of tumors [21, 22]. We reported

<sup>1</sup>Department of Pharmacology, School of Pharmacy, Qingdao University Medical College, #1 Ningde Road, Qingdao 266073, China. <sup>2</sup>Department of Gastroenterology, Xinqiao Hospital, Army Medical University, Chongqing 400037, China. <sup>3</sup>Department of General Surgery, First Hospital of Qinhuangdao, Qinhuangdao, Hebei, China. <sup>4</sup>Department of Medicine, University of California, San Diego, CA, USA. <sup>5</sup>These authors contributed equally: Hanxing Wan, Nannan Gao. ✉email: h2dong@ucsd.edu

Received: 9 May 2022 Revised: 3 July 2022 Accepted: 7 July 2022  
Published online: 26 July 2022

previously that TGF- $\beta$ -induced  $\text{Ca}^{2+}$  entry via TRPC1/NCX1 coupling to modulate  $\text{Ca}^{2+}$ -mediated motility of human pancreatic duct cells [23]. Although TRPC1 is highly expressed in human GC to likely promote GC progression [24], it is currently unknown whether TRPC1 alone or its coupling with NCX1 contributes to this process. Therefore, in the present study, we sought to investigate if NCX1 and TRPC1 are simultaneously involved in GC; and if so, what the underlying molecular mechanisms are.

## RESULTS

### Enhanced NCX1 expression in human primary GC tissues

Due to the lack of information on NCX1 expression in the stomach of normal subjects and GC patients, we first collected human primary GC tissues and corresponding adjacent tissues to compare NCX1 expression. By applying western blotting analysis, total 52 pairs of fresh gastric tissues obtained from GC patients were compared. As shown in Fig. 1, 34 pairs had higher NCX1 protein expression in human GC tissues than in adjacent tissues (Fig. 1A), accounting for 65% of the total (Fig. 1D). In contrast, 13 pairs had lower NCX1 expression in GC tissues (Fig. 1B), accounting for 25% (Fig. 1D). However, 5 pairs had no difference (Fig. 1C), accounting for 10% (Fig. 1D). Therefore, NCX1 protein expression was enhanced in human primary GC tissues.

Second, immunohistochemistry study was applied to human gastric tissues from 80 GC patients. Among these patients, their average age was 64 years old, 76% was male, 60% was diagnosed with advanced-stage (III/IV), and 74% had lymphatic metastasis (Supplementary Table 1). As shown in Fig. 1E, F, the protein expression of NCX1 was markedly enhanced in GC tissues compared to their adjacent tissues, but staining was not detected in the negative control, indicating a specific staining to NCX1 proteins. Third, the association between NCX1 expression and clinicopathologic parameters of GC progression was subsequently analyzed. As shown in Fig. 1G–I, the up-regulation of NCX1 expression was correlated with advanced clinical stage, large tumor size, and lymphatic metastasis. Furthermore, Kaplan-Meier analysis showed that the GC patients with high NCX1 expression had a poor prognosis, but those with low expression had a better prognosis (Fig. 1J). Altogether, the close association between NCX1 expression and clinicopathologic parameters strongly suggests an oncogenic role for NCX1 in human GC.

### Co-localization and binding of the enhanced NCX1 and TRPC1 in human GC cells

Since enhanced expression of TRPC1 was closely related to worse prognosis and exacerbated EMT in GC [24, 25], we first compared the expression of either TRPC1 or NCX1 proteins between 5 human GC cell lines and 1 normal gastric epithelial cell line (GES1). As shown in Fig. 1K, the expression level of NCX1 proteins was markedly enhanced in all GC cells compared to GES1 cells. Similarly, the expression level of TRPC1 proteins was also markedly enhanced in all GC cells compared to GES1 cells (Fig. 1L), suggesting both NCX1 and TRPC1 are expressed parallelly in GC cells and normal cells. Second, we performed immunofluorescence analysis to further study the expression and localization of NCX1 and TRPC1 proteins in human GC cells. As shown in Fig. 1M, both NCX1 and TRPC1 proteins were confirmed to express parallelly in 3 GC cell lines, but non-specific staining was undetected in the negative control without primary antibody. Moreover, both NCX1 and TRPC1 proteins were predominately expressed and co-localized on the plasma membrane of GC cells (Fig. 1M). Finally, our coimmunoprecipitation study clearly showed the binding of NCX1 and TRPC1 in 2 GC cell lines (Fig. 1N–Q). Therefore, the expression of NCX1 and TRPC1 is not only up-regulated but also co-localized and bound on the plasma membrane of human GC cells.

### NCX1 activation promotes proliferation, migration and invasion of human GC cells in vitro

To examine the role of NCX1 in GC, we first determined the cell proliferation of 3 human GC cell lines commonly used in the literature (MKN45, AGS and SGC7901). The varying concentrations of  $\text{CaCl}_2$  were applied to stimulate the  $\text{Ca}^{2+}$  entry mode of NCX1 since no selective activators of NCX1 are commercially available so far [26].  $\text{CaCl}_2$  at the concentrations of 0.1–2 mM, dose-dependently promoted proliferation of all GC cells (Fig. 2A, D, G), which was attenuated by KB-R7943 (Fig. 2B, E, H) and SN-6 (Supplementary Fig. 1A, B), the selective inhibitors for the  $\text{Ca}^{2+}$  entry mode of NCX1. The concentrations of KB-R7943 were chosen in the light of the different sensitivity of GC cell proliferation to the drug (Supplementary Fig. 2A–D). Similarly,  $\text{CaCl}_2$  dose-dependently promoted proliferation of CHO cells with NCX1 overexpression (CHO-NCX1) (Fig. 2P), which was attenuated by KB-R7943 (Fig. 2Q). In contrast,  $\text{CaCl}_2$  could not influence proliferation of CHO cells (CHO-K1) (Fig. 2R) and GES1 cells without NCX1 expression (Fig. 2T). Therefore,  $\text{CaCl}_2$  promotes GC cell proliferation most likely via activating the  $\text{Ca}^{2+}$  entry mode of NCX1.

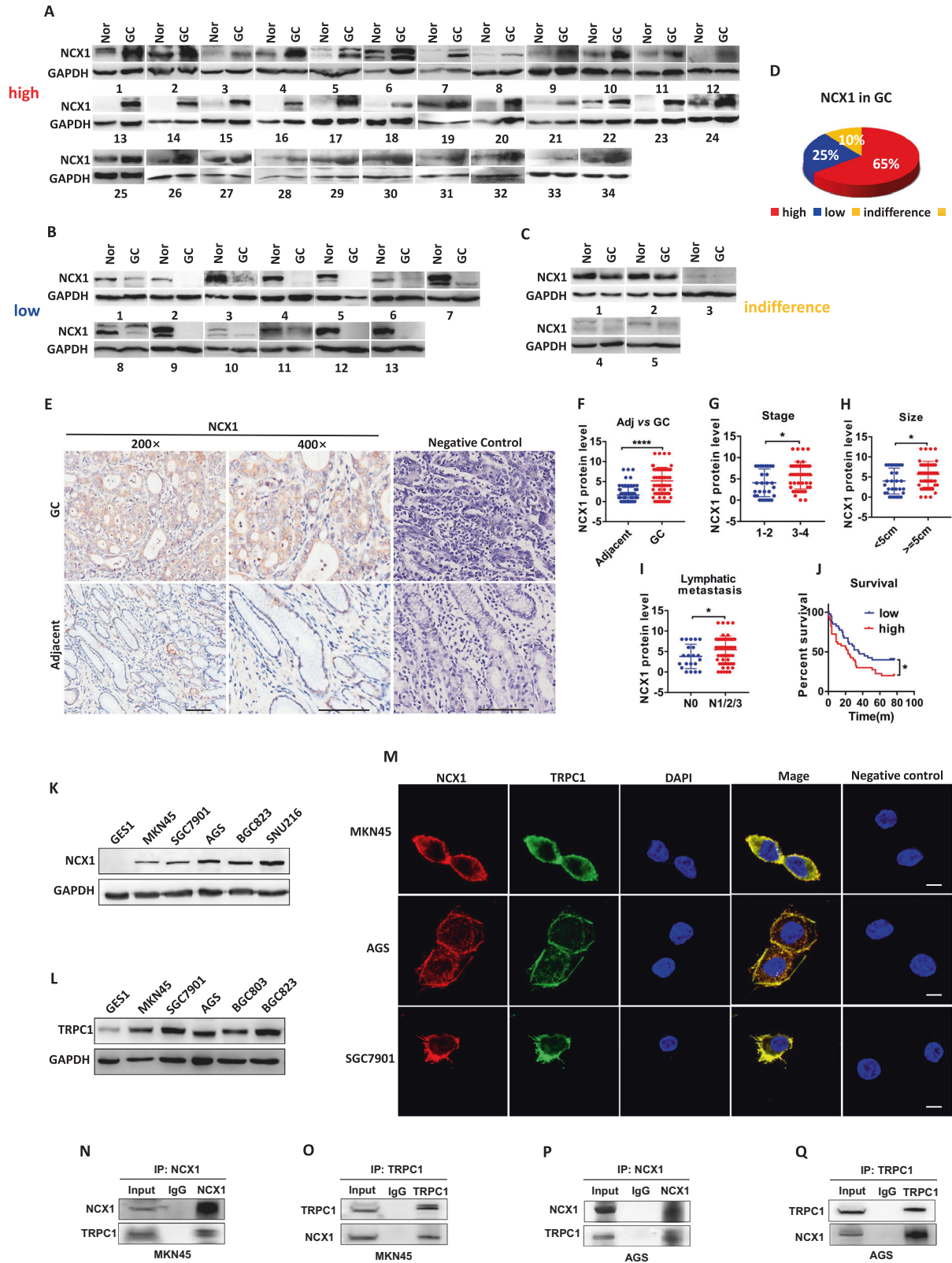
Although NCX1 enhanced migration and invasion of hepatocellular carcinoma [19], its contribution to GC progression is unknown. Second, we examined the role of NCX1 in migration and invasion of human GC cells. Cell scratch test showed that  $\text{CaCl}_2$  promoted migration of MKN45 and AGS cells, which was attenuated by KB-R7943 (Supplementary Fig. 3A, B). Moreover, transwell assays showed that  $\text{CaCl}_2$  promoted migration (Supplementary Fig. 3C, D) and invasion (Fig. 2C, F, I) of MKN45, AGS and SGC7901 cells, which were attenuated by KB-R7943 (Supplementary Fig. 3C, D and Fig. 2C, F, I). Finally, after shNCX1 was applied to successfully knock down the protein expression of NCX1 in GC cells (Fig. 3A–C),  $\text{CaCl}_2$ -induced cell proliferation (Fig. 3D, F, H), migration (Supplementary Fig. 4A–C) and invasion (Fig. 3E, G, I) were all inhibited. Taken together, NCX1 plays a critical role in GC cell proliferation, migration and invasion.

### *Hp* virulence factor promotes GC cell proliferation, migration and invasion via NCX1 activation

Since *H. pylori* infection is a pivotal risk factor for tumorigenesis of GC and ammonia/ammonium is a major *H. pylori* virulence factor,  $\text{NH}_4\text{Cl}$  was applied to the present study as a well-known ammonia/ammonium [2]. As shown in Fig. 2, like  $\text{CaCl}_2$ ,  $\text{NH}_4\text{Cl}$  dose-dependently (0.1–2 mM) promoted proliferation of MKN45, AGS and SGC7901 cells (Fig. 2J, L, N), which was attenuated by KB-R7943 (Fig. 2K, M, O). In contrast,  $\text{NH}_4\text{Cl}$  did not affect proliferation of CHO-K1 (Fig. 2S) and GES1 cells without NCX1 expression (Fig. 2U). Similarly,  $\text{NH}_4\text{Cl}$ -induced cell proliferation (Fig. 3J, L, N), migration (Supplementary Fig. 4D–F) and invasion (Fig. 3K, M, O) were all inhibited by shNCX1. Therefore, *Hp* virulence factor promotes GC cell proliferation, migration and invasion via the  $\text{Ca}^{2+}$  entry mode of NCX1.

### $\text{CaCl}_2$ , *Hp* and their virulence factors enhance NCX1 expression in GC cells

After demonstrating the promotion of  $\text{CaCl}_2$  and *Hp* virulence factors on cell proliferation, migration and invasion, we examined if they also affect NCX1 expression in GC cells. Indeed,  $\text{CaCl}_2$  enhanced NCX1 expression in MKN45, AGS and SGC7901 cells (Fig. 4A, G, M), which was attenuated by either KB-R7943 (Fig. 4B, H, N) or shNCX1 (Fig. 4C, I, O). Similarly, *H. pylori* virulence factor  $\text{NH}_4\text{Cl}$ -enhanced NCX1 expression in GC cells (Fig. 4D, J, P) was attenuated by either KB-R7943 (Fig. 4E, K, Q) or shNCX1 (Fig. 4F, L, R). Moreover, another *H. pylori* virulence factor lipopolysaccharide (LPS) [27, 28] enhanced NCX1 expression in GC cells (Fig. 4S, T, U). Finally, *H. pylori* per se also enhanced NCX1 expression (Fig. 4V, W) after co-culturing with GC cells for 24 h. However,  $\text{CaCl}_2$ ,  $\text{NH}_4\text{Cl}$ ,



LPS and *H. pylori* all did not affect NCX1 expression in GES1 cells as a negative control (Supplementary Fig. 5A–D). Taken together, these data strongly suggest that like  $CaCl_2$ , *H. pylori* per se and their virulence factors promote GC through enhancing NCX1 expression as well.

**NCX1 coordinates with TRPC1 to promote GC cell proliferation and migration**

TRPC family is a potential partner for the  $Ca^{2+}$  entry mode of NCX1 [29]. Among them, TRPC1 and TRPC6 were highly expressed in human GC to play an oncogenic role in GC progression [24, 30].



**Fig. 1 The enhanced expression of NCX1 and TRPC1 in human primary gastric cancer tissues and cells.** Western blot analysis applied to compare the expression levels of NCX1 proteins between gastric cancer (GC) tissues and adjacent normal (Nor) tissues from 52 GC patients: 34 pairs with high expression (A), 13 pairs with low expression (B), and 5 pairs without difference (C). D Summary data showing the percentage of high, low and indifference of NCX1 expression in GC tissues compared to adjacent tissues. E, F Representative and summary data of immunohistological staining on NCX1 proteins in GC tissues compared to adjacent tissues. Scale bar=100 μm for each image. Negative control: without primary antibody. (\*\*\*\* $P < 0.0001$ ,  $n = 80$  patients). Relative NCX1 protein levels in GC tissues from the patients with different stages (G), tumor sizes (H), and lymphatic metastasis (I). ( $P < 0.05$ ,  $n = 80$  patients). J Kaplan–Meier analysis of survival ratio of GC patients with low and high NCX1 expression levels ( $P < 0.05$ ,  $n = 80$  patients). K, L Western blot analysis of NCX1 and TRPC1 protein levels in GES1 and GC cell lines. M Immunofluorescence staining images of NCX1 and TRPC1 proteins with primary antibody and without the antibody (negative control) in MKN45, AGS and SGC7901 cells. Scale bar=10 μm for each image. N–Q Co-immunoprecipitation showing the binding of NCX1 and TRPC1 proteins in GC cells.

We therefore focused on a possible coupling of TRPC1/6 and NCX1 in GC development. TRPC6 antagonist SAR7334 did not affect  $\text{CaCl}_2$ -promoted GC cell proliferation (Supplementary Fig. 1C, D), excluding the involvement of TRPC6. However, as shown in Fig. 5,  $\text{CaCl}_2$ -induced GC cell proliferation and migration were attenuated by either KB-R7943 or a TRPC1 blocker SKF96365, which concentrations were chosen based on its sensitivity (Supplementary Fig. 2E–G). Moreover, the  $\text{CaCl}_2$ -induced cell proliferation and migration were further attenuated by a combination of the selective inhibitors for both NCX1 and TRPC1 (Fig. 5A–C, G–I). Similarly, the  $\text{CaCl}_2$ -induced cell proliferation and migration were further attenuated by a combination of shNCX1 plus SKF96365 (Fig. 5D–F, J–L). Taken together, these data strongly suggest that NCX1 coordinate with TRPC1 to promote GC cell proliferation and migration.

#### **Hp virulence factor could stimulate TRPC1 channels to trigger $\text{Ca}^{2+}$ entry mode of NCX1 in GC cells**

We next applied cell  $\text{Ca}^{2+}$  imaging to determine if NCX1 operates in  $\text{Ca}^{2+}$  entry mode to induce  $[\text{Ca}^{2+}]_{\text{cyt}}$  increase in GC cells. First, extracellular  $0 \text{ Na}^+$  that triggers  $\text{Ca}^{2+}$  entry mode of NCX1 significantly induced  $[\text{Ca}^{2+}]_{\text{cyt}}$  signaling in  $\text{Ca}^{2+}$ -containing solutions but not in  $\text{Ca}^{2+}$ -free solutions (Fig. 6A). Second,  $0 \text{ Na}^+$ -induced  $[\text{Ca}^{2+}]_{\text{cyt}}$  signaling in  $\text{Ca}^{2+}$ -containing solutions was abolished by KB-R7943 (Fig. 6B). Third,  $0 \text{ Na}^+$  also markedly increased  $[\text{Ca}^{2+}]_{\text{cyt}}$  signaling in CHO-NCX1 cells with NCX1 overexpression (Fig. 6G, I, J), but not in CHO-K1 cells without NCX1 overexpression (Fig. 6H–J). These data strongly support NCX1 operates in  $\text{Ca}^{2+}$  entry mode in GC cells like in CHO-NCX1 cells. We examined if  $\text{NH}_4\text{Cl}$  and the local acidic micro-environment in *Hp* infection-induced chronic inflammation and tumorigenesis could stimulate NCX1 activity. Like  $0 \text{ Na}^+$ ,  $\text{NH}_4\text{Cl}$  and acid (pH 4.5) indeed had similar stimulation on  $\text{Ca}^{2+}$  entry mode of NCX1 in SGC7901 cells (Fig. 6C–F).

We further examined if TRPC1/NCX1 coupling mediates  $\text{Ca}^{2+}$  signaling in GC cells since NCX1 operation in  $\text{Ca}^{2+}$  entry mode requires  $\text{Na}^+$  entry via TRPC channels [29]. After shTRPC1 successfully knocked down TRPC1 expression in GC cells (Fig. 6N, R), both  $0 \text{ Na}^+$ - and  $\text{NH}_4\text{Cl}$ -induced  $\text{Ca}^{2+}$  signaling was almost abolished (Fig. 6K–M, O–Q). These data verify that *Hp* virulence factor induces  $\text{Ca}^{2+}$  signaling via TRPC1/NCX1 coupling in GC cells.

#### **NCX1 activation promotes GC through AKT/ $\beta$ -catenin pathway**

We next elucidated NCX1-promoted oncogenic mechanisms. Since AKT/ $\beta$ -catenin pathway plays a crucial role in the development of GC [31] and colorectal cancer [32], and aberrant  $[\text{Ca}^{2+}]_{\text{cyt}}$  promoted GC through this pathway [11], we therefore examined the role of AKT/ $\beta$ -catenin. First, after NCX1 was activated by  $\text{CaCl}_2$ , both AKT phosphorylation (Ser473) and  $\beta$ -catenin phosphorylation (Ser675) were increased in MKN45 and AGS cells (Fig. 7A, B, E, F, I, J, M, N). Second, the  $\text{CaCl}_2$ -induced phosphorylation of AKT and  $\beta$ -catenin were attenuated by either KB-R7943 (Fig. 7A, B, E, F) or NCX1 knockdown (Fig. 7I, J, M, N). Third,  $\text{NH}_4\text{Cl}$  also increased AKT phosphorylation (Ser473) and  $\beta$ -catenin phosphorylation (Ser675)

in MKN45 and AGS cells (Fig. 7C, D, G, H, K, L, O, P), which were attenuated by KB-R7943 (Fig. 7C, D, G, H) and NCX1 knockdown (Fig. 7K, L, O, P). Therefore, both  $\text{CaCl}_2$ - and  $\text{NH}_4\text{Cl}$ -induced NCX1 activation could stimulate phosphorylation of AKT and  $\beta$ -catenin in GC cells.

#### **NCX1 couples with TRPC1 to promote GC through AKT pathway**

Since the  $\text{Ca}^{2+}$  entry mode of NCX1 usually functions via a coupling with TRPC1 [29], we investigated whether TRPC1 channels are involved in NCX1-mediated AKT phosphorylation. Western blotting analysis exhibited that after  $\text{CaCl}_2$  induced AKT phosphorylation in GC cells, either NCX1 inhibitor KB-R7943 or TRPC1 inhibitor SKF96365 significantly attenuated the  $\text{CaCl}_2$ -induced AKT phosphorylation; but both of them further attenuated it (Fig. 8A, D). Moreover, either a combination of shNCX1 and SKF96365 (Fig. 8B, E) or a combination of shTRPC1 and KB-R7943 (Fig. 8C, F) further attenuated the  $\text{CaCl}_2$ -induced AKT phosphorylation. These data verify TRPC1/NCX1 coupling enhances AKT phosphorylation in GC cells.

#### **NCX1 activation enhances GC growth and metastasis in vivo**

We applied subcutaneously xenografted GC model of nude mice to verify the oncogenic role of the  $\text{Ca}^{2+}$  entry mode of NCX1 in GC growth in vivo. NCX1 activation by  $\text{CaCl}_2$  increased tumor weights (Fig. 8G), which was attenuated by KB-R7943 (Fig. 8H). Moreover, the knockdown of NCX1 in SGC-7901 cells by NCX1-shRNA lentiviruses markedly suppressed GC growth (Fig. 8I). Immunohistochemical analysis showed that the tumors derived from the implants pre-treated with NCX1-shRNA lentiviruses had lower expression of NCX1 and Ki67 than those pre-treated with control shRNA (Fig. 8K, L, M). Therefore, NCX1 promotes GC growth in vivo.

We further applied abdominal transplantation tumor model of nude mice to verify NCX1-promoted GC metastasis in vivo. As shown in Fig. 8J,  $\text{CaCl}_2$ -induced GC metastasis was markedly suppressed by pretreatment with NCX1-shRNA lentiviruses. Compared to NC group, tumor numbers in the group pretreatment with NCX1-shRNA were decreased by about 50%. Therefore, NCX1 promotes GC metastasis in vivo as well.

#### **DISCUSSION**

In the present study, we demonstrate for the first time that NCX1 and TRPC1 simultaneously participate in GC development. Several lines of evidence suggest that NCX1 promotes human GC growth and metastasis by a novel coupling to TRPC1 channels. First, the expression of NCX1 and TRPC1 was enhanced in human primary GC tissues and most GC cell lines. Second, the enhanced NCX1 expression was closely correlated with poor progression and survival of GC patients. Third, NCX1 and TRPC1 were co-expressed in parallel, co-localized and bound on the membrane of GC cells. Forth, co-stimulation of NCX1 and TRPC1 with  $\text{CaCl}_2$  and *Hp* virulence factors promoted GC cell proliferation, migration and invasion in vitro, and increased gastric tumor size, number and



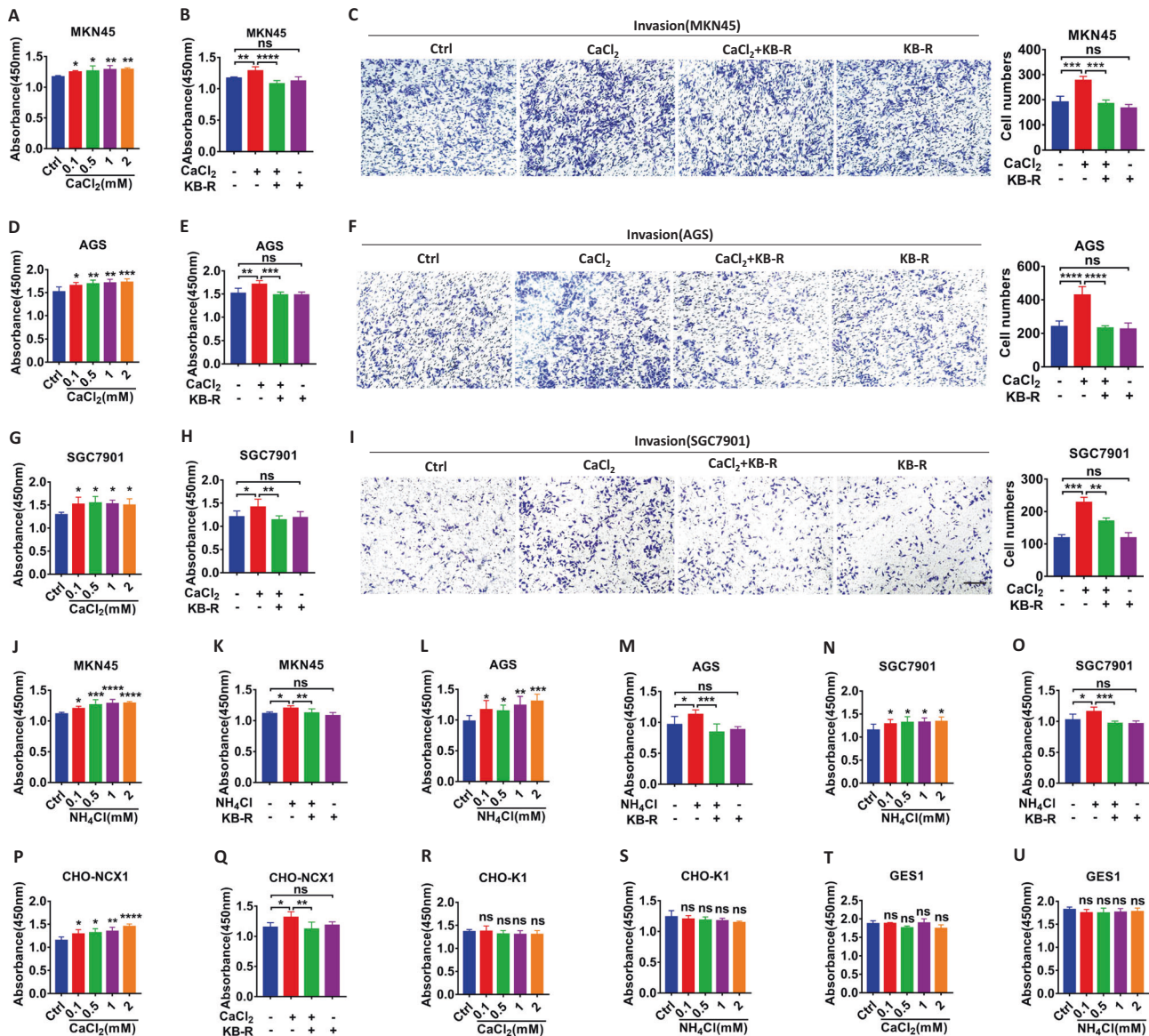


**Fig. 2** NCX1 activation promotes proliferation and invasion of human GC cells. Dose-dependently enhanced proliferation of CaCl<sub>2</sub> (0.1–2 mM) in MKN45 (A), AGS (D), and SGC7901 (G) cells. The inhibitory effect of KB-R7943 (KB-R, 1 μM in MKN45, 4 μM in AGS, 8 μM in SGC7901) on CaCl<sub>2</sub> (1 mM)-induced proliferation (B, E, H) and invasion (C, F, I) of GC cells, Scale bar=200 μm for each image. Dose-dependently enhanced proliferation of NH<sub>4</sub>Cl (0.1–2 mM) in MKN45 (J), AGS (L), and SGC7901 (N) cells, and the inhibitory effect of KB-R7943 on NH<sub>4</sub>Cl (1 mM)-induced proliferation of MKN45 (K), AGS (M), and SGC7901 (O) cells. P, Q Dose-dependently enhanced proliferation of CaCl<sub>2</sub> (0.1–2 mM) in CHO-NCX1 with NCX1 overexpression, and the inhibitory effect of KB-R7943 (0.2 μM) on CaCl<sub>2</sub> (1 mM)-induced proliferation of CHO-NCX1 cells. R–U No effects of CaCl<sub>2</sub> (0.1–2 mM) and NH<sub>4</sub>Cl (0.1–2 mM) on proliferation of CHO-K1 without NCX1 overexpression and GES1 cells. (\**P* < 0.05, \*\**P* < 0.01, \*\*\**P* < 0.001, \*\*\*\**P* < 0.0001, *n* = 3; ns, no significant differences).

peritoneal dissemination in vivo. Fifth, by coupling with TRPC1, NCX1 operated in Ca<sup>2+</sup> entry mode to promote GC through AKT/β-catenin signaling pathway.

NCX1 plays a critical role in mediating [Ca<sup>2+</sup>]<sub>cyt</sub> homeostasis in various types of human cells [12]; however, it was investigated predominately in the cardiovascular, nervous, and renal systems instead of GI tract [13]. Nothing is currently known about NCX1 in gastric epithelia even though it is expressed in gastric smooth muscle to likely mediate motility [33]. We revealed previously that NCX1 not only physiologically mediates lower esophageal sphincter relaxation [34] and intestinal epithelial ion transports [35], but also pathologically involves in GI inflammation and cancer [18, 36]. Disruption of [Ca<sup>2+</sup>]<sub>cyt</sub> homeostasis induced by the enhanced Ca<sup>2+</sup> entry mode of NCX1 has been detected in several cancer, such as pancreatic cancer [36], breast cancer [37],

glioblastoma [38], and melanoma [39]. Although we have demonstrated the roles of NCX1-mediated Ca<sup>2+</sup> signaling in esophageal cancer [18], pancreatic cancer [36] and hepatocellular carcinoma [19], the pathological roles of NCX1 in the stomach, especially in GC development remain totally unexplored. In the present study, we verified the enhanced NCX1 expression in human primary GC tissues and cells; and the enhanced NCX1 expression was correlated with larger tumor size, higher histological grade, lymphatic metastasis, advanced clinical stage and poor prognosis, which strongly suggests NCX1 as a potential marker for GC prognosis.

We have provided experimental data to support a pivotal oncogenic role of NCX1 in *Hp*-associated GC since its activation with either calcium or *Hp* virulence factors promoted GC cell proliferation, invasion and metastasis in vitro and in vivo.

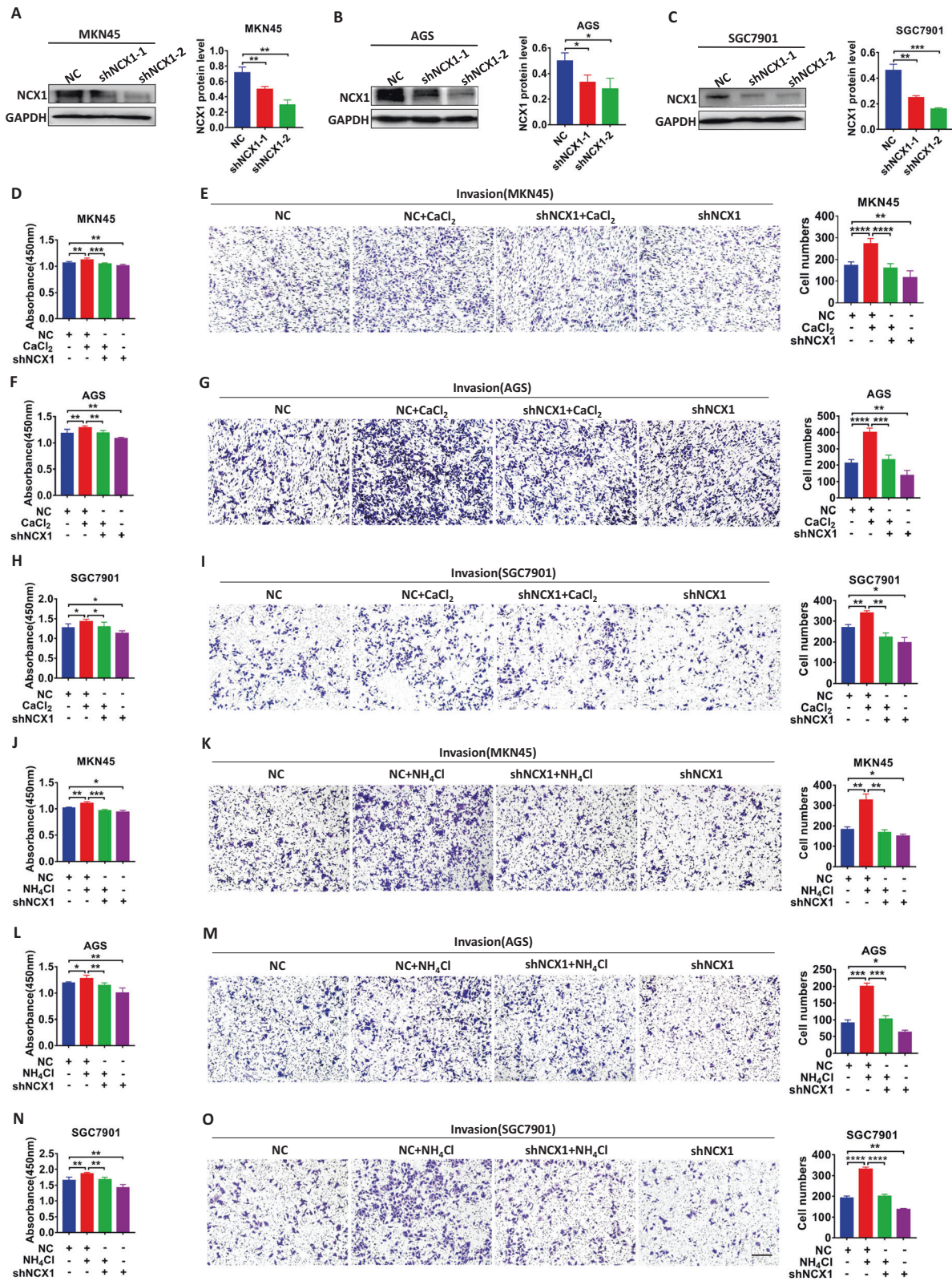


**Fig. 3**  $\text{CaCl}_2$  and  $\text{NH}_4\text{Cl}$  promote proliferation and invasion of human GC cells through NCX1 activation. Representative images of NCX1 protein expression in GC cells with NCX1 knockdown and summary data of NCX1 protein levels in MKN45 (A), AGS (B), and SGC7901 (C) cells ( $P < 0.05$ ,  $^*P < 0.01$ ,  $^{***}P < 0.001$ , vs. NC,  $n = 3$ ). The effect of shNCX1 on  $\text{CaCl}_2$  (1 mM)-induced proliferation (D, F, H) and invasion (E, G, I) of GC cells. The effect of shNCX1 on  $\text{NH}_4\text{Cl}$  (1 mM)-induced proliferation (J, L, N) and invasion (K, M, O) of GC cells. Scale bar = 200  $\mu\text{m}$  for each image. ( $^*P < 0.05$ ,  $^{**}P < 0.01$ ,  $^{***}P < 0.001$ ,  $^{****}P < 0.0001$ ,  $n = 3$ ; ns, no significant differences).



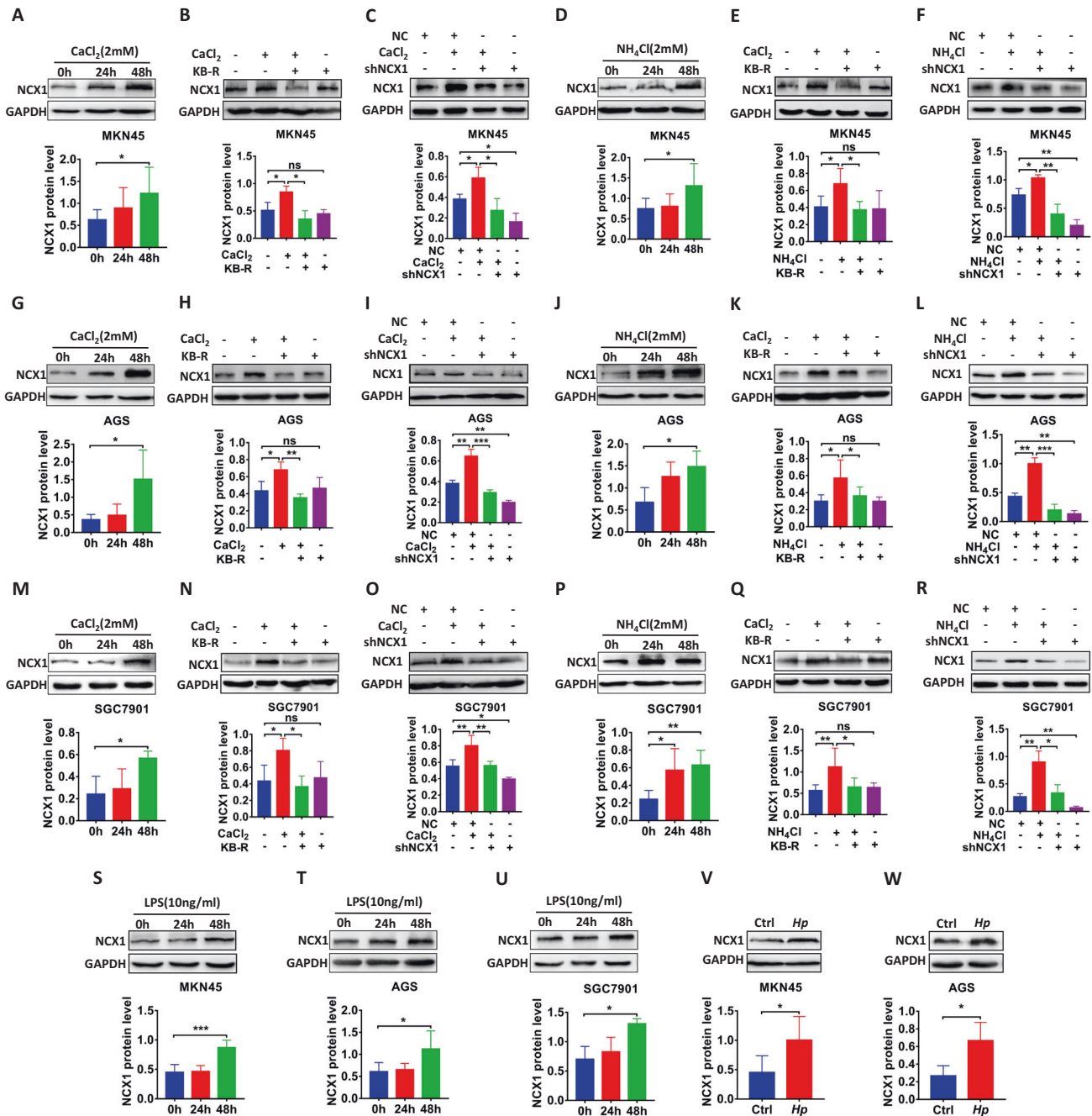


**Fig. 4**  $\text{CaCl}_2$ , *Hp* and virulence factors enhance NCX1 expression in human GC cells. **A, G, M** Representative time courses of  $\text{CaCl}_2$  (2 mM)-enhanced NCX1 protein expression in GC cells. Inhibitory effect of KB-R7943 (KB-R, 1  $\mu\text{M}$  in MKN45, 4  $\mu\text{M}$  in AGS, 8  $\mu\text{M}$  in SGC7901) (**B, H, N**) or shNCX1 (**C, I, O**) on  $\text{CaCl}_2$  (2 mM)-enhanced NCX1 expression in GC cells. **D, J, P** Representative time courses of  $\text{NH}_4\text{Cl}$  (2 mM)-enhanced NCX1 protein expression in GC cells. Inhibitory effect of KB-R7943 (**E, K, Q**) or shNCX1 (**F, L, R**) on  $\text{NH}_4\text{Cl}$  (2 mM)-enhanced NCX1 protein expression in GC cells. **S, T, U** Representative time courses LPS (10 ng/ml)-enhanced NCX1 protein expression in GC cells. **V, W** Representative time courses *H. pylori*-enhanced NCX1 protein in GC cells. (\* $P < 0.05$ , \*\* $P < 0.01$ , \*\*\* $P < 0.001$ ,  $n = 3$ ; ns, no significant differences).

Consistently, both selective blocker for the  $\text{Ca}^{2+}$  entry mode of NCX1 and its specific knockdown attenuated the oncogenic effects of NCX1. Therefore, NCX1 may play a general oncogenic role in GI cancer, such as in GC reported here and in esophageal cancer [18], pancreatic cancer [36] and hepatocellular carcinoma [19] reported previously. Moreover, TRP channels also play different roles in GC development [9–11]. Although the enhanced TRPC1 is likely involved in GC progression [24], its association with NCX1 is unknown. Here we revealed not only enhanced TRPC1 expression but also its co-localization and binding with NCX1 in

human GC cells. Importantly, TRPC1-promoted GC cell proliferation and migration were attenuated by TRPC1 channel blocker. Therefore, in parallel with NCX1, TRPC1 also plays an oncogenic role in GC.

Under physiological status, NCX1 primarily functions in  $\text{Ca}^{2+}$  exit mode; however, under some pathological conditions (such as in tumorigenesis), NCX1 is switched to  $\text{Ca}^{2+}$  entry mode to allow sustained  $\text{Ca}^{2+}$  entry [12]. Most reports have suggested TRPC as a potential partner for NCX mode switch in non-excitable cells (such as GC cells) [29].  $\text{Na}^+$  could enter through TRPC channels to raise



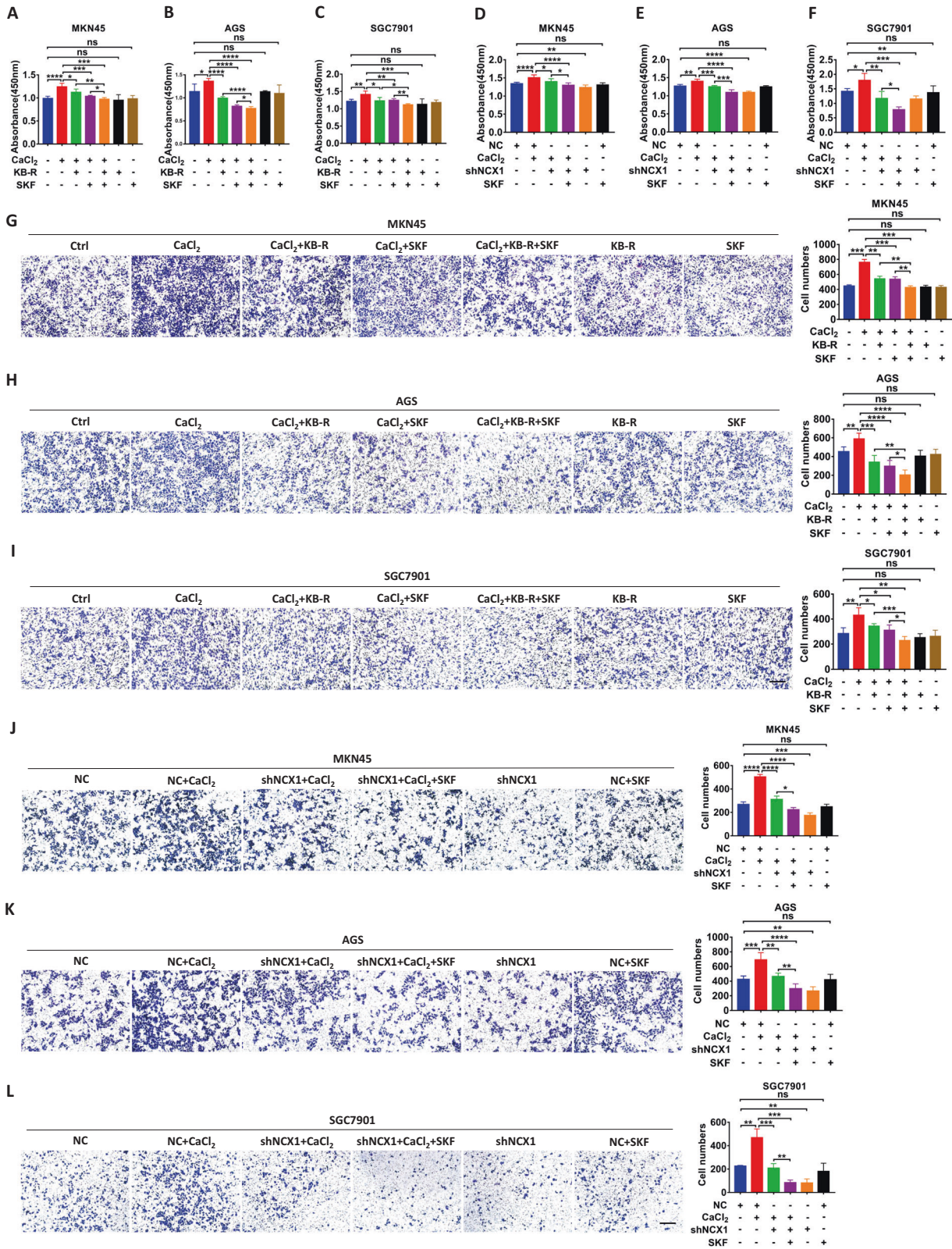
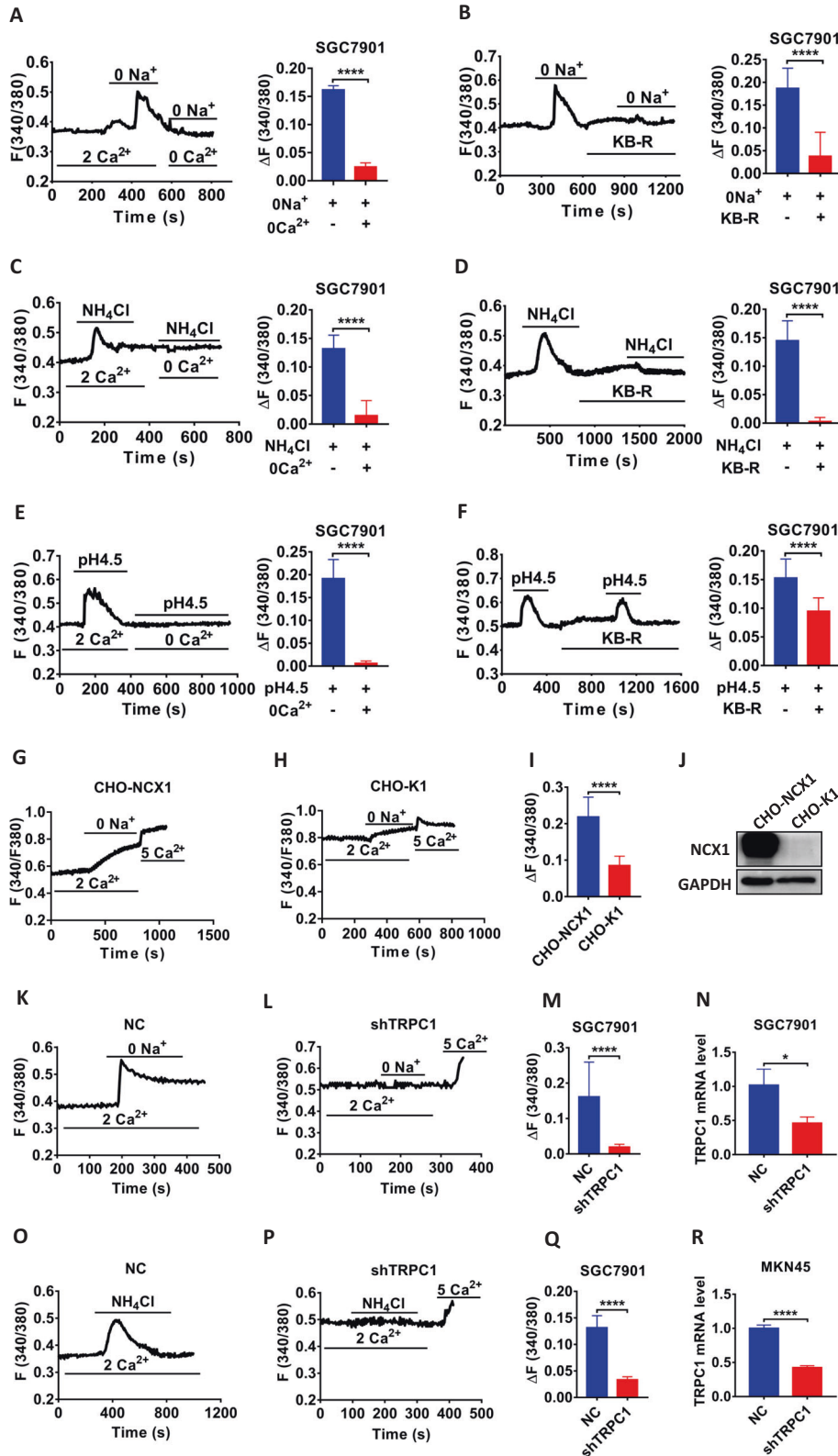


**Fig. 5 NCX1 coordinates with TRPC1 to promote proliferation and migration of human GC cells.** Summary data showing the inhibitory effects of either KB-R7943 (KB-R, 1  $\mu$ M in MKN45, 4  $\mu$ M in AGS, 8  $\mu$ M in SGC7901), SKF96365 (SKF, 1  $\mu$ M) or KB-R plus SKF on CaCl<sub>2</sub> (1 mM)-enhanced proliferation (A–C) and migration (G–I) of GC cells. D–F, J–L Summary data showing the inhibitory effect of either shNCX1, SKF96365 (SKF, 1  $\mu$ M) or shNCX1 plus SKF on CaCl<sub>2</sub> (1 mM)-enhanced proliferation and migration of GC cells. Scale bar = 200  $\mu$ m for each image. (\* $P$  < 0.05, \*\* $P$  < 0.01, \*\*\* $P$  < 0.001, \*\*\*\* $P$  < 0.0001,  $n$  = 3; ns, no significant differences).



$[Na^+]_{cyt}$  under the restricted membrane space and induce membrane depolarization, switching NCX1 to  $Ca^{2+}$  entry mode [29]. Indeed, in the present study we revealed a novel coupling of TRPC1 and the  $Ca^{2+}$  entry mode of NCX1 in GC development because: 1) both NCX1 and TRPC1 play similar oncogenic roles in GC; 2) GC cell proliferation and migration could be further

attenuated by a combination of selective blockers and specific knockdown of NCX1 and TRPC1; 3)  $CaCl_2$  and *Hp* virulence factors could stimulate TRPC1 and NCX1 coupling to induce  $Ca^{2+}$  signaling; 4) a protein-protein interaction of TRPC1 and NCX1 is verified in GC cells. Therefore, due to a general existence of TRPC and NCX1 coupling in GC, pancreatic cancer [23], and

**Fig. 6** *Hp* virulence factor and acid stimulate NCX1/TRPC1 coupling in human GC cells. Summary tracings of  $[Ca^{2+}]_{cyt}$  time courses in response to extracellular 0 Na<sup>+</sup> (A), NH<sub>4</sub>Cl (5 mM) (C) and pH 4.5 (E) in the presence of extracellular 2 Ca<sup>2+</sup> or 0 Ca<sup>2+</sup> (left). Summary data showing the peaks of 0 Na<sup>+</sup>, NH<sub>4</sub>Cl and pH 4.5-increased  $[Ca^{2+}]_{cyt}$  signaling in SGC7901 cells (right) (A, *n* = 20 cells; C, *n* = 11 cells; E, *n* = 11 cells, \*\*\*\**P* < 0.0001). Summary tracings of  $[Ca^{2+}]_{cyt}$  time courses in response to 0 Na<sup>+</sup> (B), NH<sub>4</sub>Cl (5 mM) (D) and pH 4.5 (F) in the presence of 2 Ca<sup>2+</sup> or 2 Ca<sup>2+</sup> plus KB-R7943 (KB-R, 30 μM) (left). Summary data showing the peaks of 0 Na<sup>+</sup>, NH<sub>4</sub>Cl and pH 4.5-increased  $[Ca^{2+}]_{cyt}$  signaling in SGC7901 cells (right) (B, *n* = 20 cells; D, *n* = 23 cells; F, *n* = 26 cells, \*\*\*\**P* < 0.0001). Summary tracings of  $[Ca^{2+}]_{cyt}$  time courses in response to 0 Na<sup>+</sup> in the presence of 2 Ca<sup>2+</sup> or 5Ca<sup>2+</sup> in CHO-NCX1 (G) and CHO-K1 (H) cells. I Summary data showing the peaks of 0 Na<sup>+</sup>-increased  $[Ca^{2+}]_{cyt}$  signaling described as in G, H (G, *n* = 23 cells; H, *n* = 17 cells, \*\*\*\**P* < 0.0001). J Western blot analysis of NCX1 protein levels in CHO-NCX1 and CHO-K1 cells. Summary tracings of  $[Ca^{2+}]_{cyt}$  time courses in response to 0 Na<sup>+</sup> (K, L) and NH<sub>4</sub>Cl (5 mM) (O, P) in the presence of 2 Ca<sup>2+</sup> in NC (K, O) or shTRPC1 (L, P) of SGC7901 cells. Summary data showing the peaks of 0 Na<sup>+</sup> (M) or NH<sub>4</sub>Cl (Q)-increased  $[Ca^{2+}]_{cyt}$  signaling described as in K, L, O, P (*n* = 11 cells, \*\*\*\**P* < 0.0001). N, R RT-PCR analysis of TRPC1 mRNA levels in NC and shTRPC1 of GC cells (*n* = 3, \**P* < 0.05, \*\*\*\**P* < 0.0001). Each one is 3 independent experiments with similar results.

hepatocellular carcinoma [19], this coupling could allow aberrant sustained Ca<sup>2+</sup> entry to promote most digestive cancer.

It has been well documented that aberrant Ca<sup>2+</sup> signaling participates in chronic inflammation and cancer, such as GC developed from *Hp*-associated gastric inflammation [40]. Moreover, limuro et al. found that dietary calcium enhances the *Hp*-induced gastritis in Mongolian gerbils [41]; in contrast, calcium channel blockers attenuate chemically induced gastritis and GC in rats [42, 43]. Consistently with our previous report on the oncogenic role of calcium in GC development [11], here we further reveal that CaCl<sub>2</sub> and *Hp* virulence factors enhance the expression, activity and coupling of NCX1 and TRPC1 to promote GC development, strongly suggesting a critical role of TRPC1/NCX1-mediated aberrant Ca<sup>2+</sup> signaling in *Hp*-associated GC.

Our results indicate the TRPC1/NCX1-mediated Ca<sup>2+</sup> signaling increases AKT and β-catenin phosphorylation in GC cells, which supports our notion that TRPC1/NCX1 coupling induces GC development through the Ca<sup>2+</sup>/AKT/β-catenin pathway (Fig. 8N), further confirming the pivotal role of this pathway in GC as in our previous report [11]. Therefore, our findings strongly suggest not only that aberrant Ca<sup>2+</sup> entry could promote GC via Ca<sup>2+</sup>/AKT/β-catenin pathway, but also that calcium supplement and *Hp* infection are likely synergistic risk factors for GC pathogenesis.

In conclusion, we demonstrate for the first time that TRPC1/NCX1 coupling promotes *Hp*-associated GC development. Mechanistically, TRPC1/NCX1 coupling-mediated aberrant Ca<sup>2+</sup> entry activates AKT/β-catenin pathway to consequently promote GC. Although NCX and TRP channels represent a relatively new field of cancer research with most studies still in their infancy, they hold tremendous potentials that have yet to be uncovered in the hopes of achieving major clinical breakthroughs in GC therapy. Particularly, due to a critical role of the Ca<sup>2+</sup> exit mode of NCX1 under physiological status, targeting TRPC1/NCX1 coupling could be a novel strategy for selectively blocking the Ca<sup>2+</sup> entry mode of NCX1 to potentially treat if not all solid cancers but at least digestive cancer with less side effect.

## MATERIALS AND METHODS

### Ethics statement and human tissue samples

All animal and clinical studies were approved by the Clinical Research Ethics Committee of the Qingdao University Medical College, Qingdao and Army Medical University (AMU), Chongqing, China. 52 pairs of GC and adjacent tissues for western blotting were collected from the surgical patients in Xinqiao Hospital of the AMU and all resected specimens were confirmed by pathological examination. Informed consent was obtained for all patients. All animal care and experimental procedures complied with the "Guide for the Care and Use of Laboratory Animals" published by the National Institutes of Health, USA. Animal studies are reported in compliance with the ARRIVE guidelines [44].

### Cell culture

The human gastric normal epithelial mucosa cell line (GES1) and gastric cancer cell lines MKN45, SGC7901, AGS, BGC803, BGC823 and SNU216 were purchased from Chinese Academy of Sciences (Shanghai, China). The

CHO cells with NCX1 overexpression and CHO-K1 cells without NCX1 overexpression were kindly provided by the University of California, San Diego, California, USA [34]. All cells were maintained in RPMI-1640, DMEM-HIGH GLUCOSE or F-12 medium (HyClone, USA) supplemented with 10% fetal bovine serum (HyClone, USA) and 1% penicillin/streptomycin (Invitrogen, USA) in a 37 °C humidified atmosphere containing 5% CO<sub>2</sub>.

### Preparation and infection of lentiviruses

Lentiviruses were purchased from HANBIO (Shanghai, China). The sequences for NCX1 shRNA, TRPC1 shRNA and NC were described in the supplemental materials. GC cells were infected with lentiviruses according to the protocol of the manufacturer.

### Quantitative real-time PCR

Quantitative real-time PCR was performed as previously described [9, 10]. All samples were run in triplicate, and β-actin was used as an internal control. Primers were described in the supplemental materials.

### Western blotting

Western blotting was performed as previously described [9, 10]. The antibodies were described in the supplemental materials.

### Co-immunoprecipitation and immunohistochemistry

Co-immunoprecipitation [45, 46] and immunohistochemistry [9, 11] were performed as previously described. The antibodies of co-immunoprecipitation are anti-TRPC1 (No. ACC-010, alomone labs, Israel) and anti-NCX1 (No. ANX-011, alomone labs, Israel). The GC and adjacent tissue microarray for immunostaining were purchased from SHANGHAI OUTDO BIOTECH CO., LTD (Shanghai, China). The tissue samples were incubated with anti-NCX1 (No. N216, Sigma, USA). The degree of staining in the NCX1 sections was observed and scored by two pathologists. According to previously defined criteria by T. Takenoue et al. [47], the percentage of NCX1 positivity was scored from 0 to 4 as follows: 0, <5%; 1, 5–25%; 2, 26–50%; 3, 51–75%; 4, >=76%. The intensity of immunostaining was scored as: 0 (no staining); 1 (weak); 2 (moderate); and 3 (intense). Subsequently, the two scores were multiplied and the product was defined as immunohistochemical score. Accordingly, the final expression level of NCX1 was defined as low (0–4) and high (5–12). The IHC of mice tissue samples were incubated with anti-NCX1 (No. ANX-011, alomone labs, USA) and anti-Ki67 (No. ab15580, Abcam, UK), and the staining section were performed as previously described [10].

### Immunofluorescence assay

After fixed and blocked, the GC cells were incubated with anti-NCX1 antibody (No. MA3-926, Invitrogen) overnight at 4 °C. Next, the cells were incubated with Cy3 labeled anti-mouse (No. A0521, Beyotime, China) secondary antibody for 1 h at room temperature. Then cells were incubated with anti-TRPC1 antibody (No. ACC-010, alomone labs, Israel) and 647 labeled anti-rabbit (No. A0468, Beyotime, China) secondary antibody for 1 h at room temperature respectively. Finally, nuclei were stained with DAPI for 5 min and images were captured using confocal microscope.

### Cell proliferation and scratch assays

Cell proliferation assay was performed as previously described [9]. Cell proliferation was measured by CCK8 assay (No. C0038, Beyotime Biotechnology, China) according to the protocol of the manufacturer. Cell



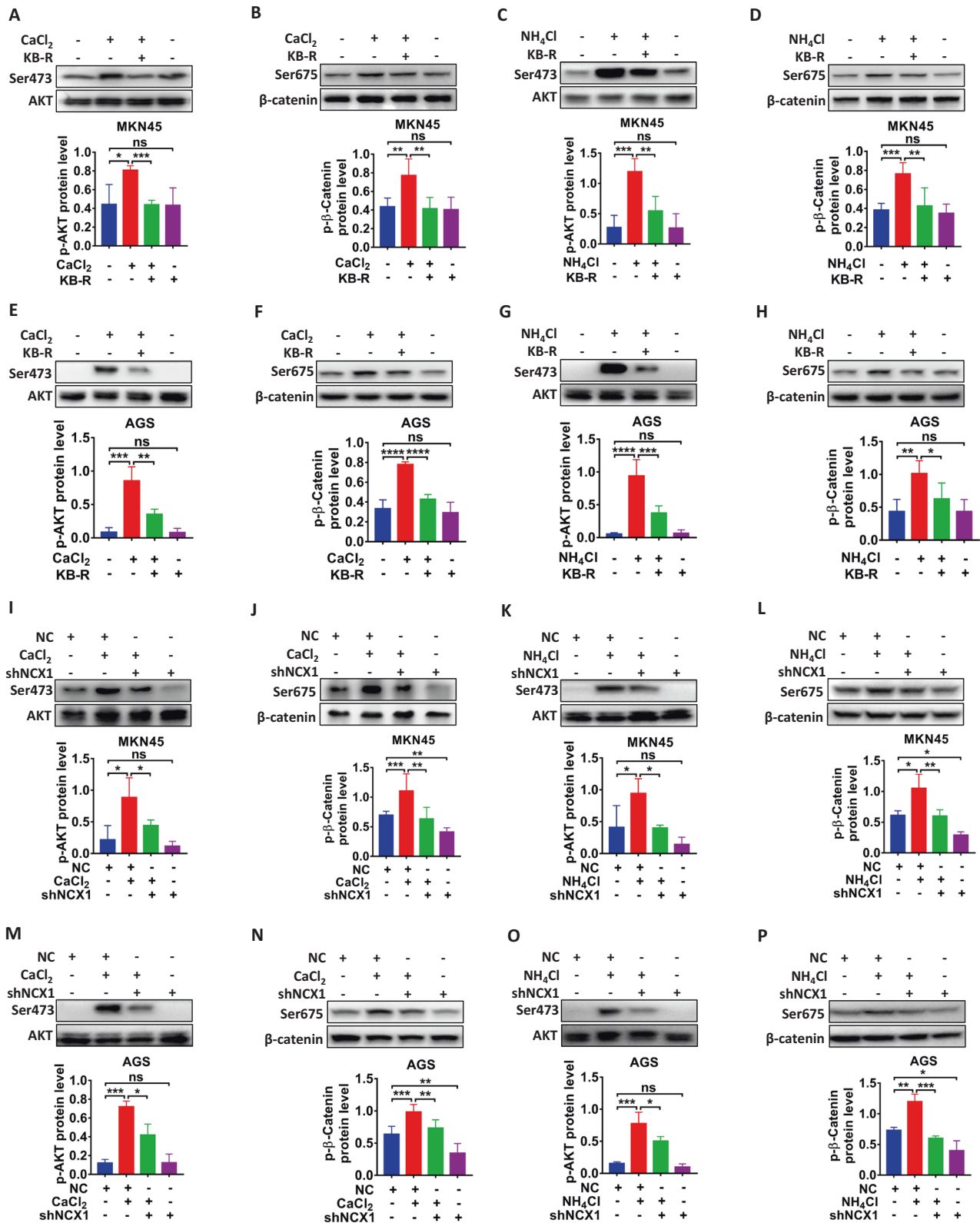


**Fig. 7** NCX1 activation induces phosphorylation of AKT and  $\beta$ -catenin in human GC cells. **A, B, E, F** Inhibitory effect of KB-R7943 (KB-R, 1  $\mu$ M in MKN45, 4  $\mu$ M in AGS) on CaCl<sub>2</sub> (2 mM)-induced AKT and  $\beta$ -catenin phosphorylation in MKN45 and AGS cells. **C, D, G, H** Inhibitory effect of KB-R7943 on NH<sub>4</sub>Cl (2 mM)-induced AKT and  $\beta$ -catenin phosphorylation in MKN45 and AGS cells. **I, J, M, N** Inhibitory effect of shNCX1 on CaCl<sub>2</sub>-induced AKT and  $\beta$ -catenin phosphorylation in MKN45 and AGS cells. **K, L, O, P** Inhibitory effect of shNCX1 on NH<sub>4</sub>Cl-induced AKT and  $\beta$ -catenin phosphorylation in MKN45 and AGS cells. ( $^*P < 0.05$ ,  $^{**}P < 0.01$ ,  $^{***}P < 0.001$ ,  $^{****}P < 0.0001$ ,  $n = 3$ ; ns, no significant differences).

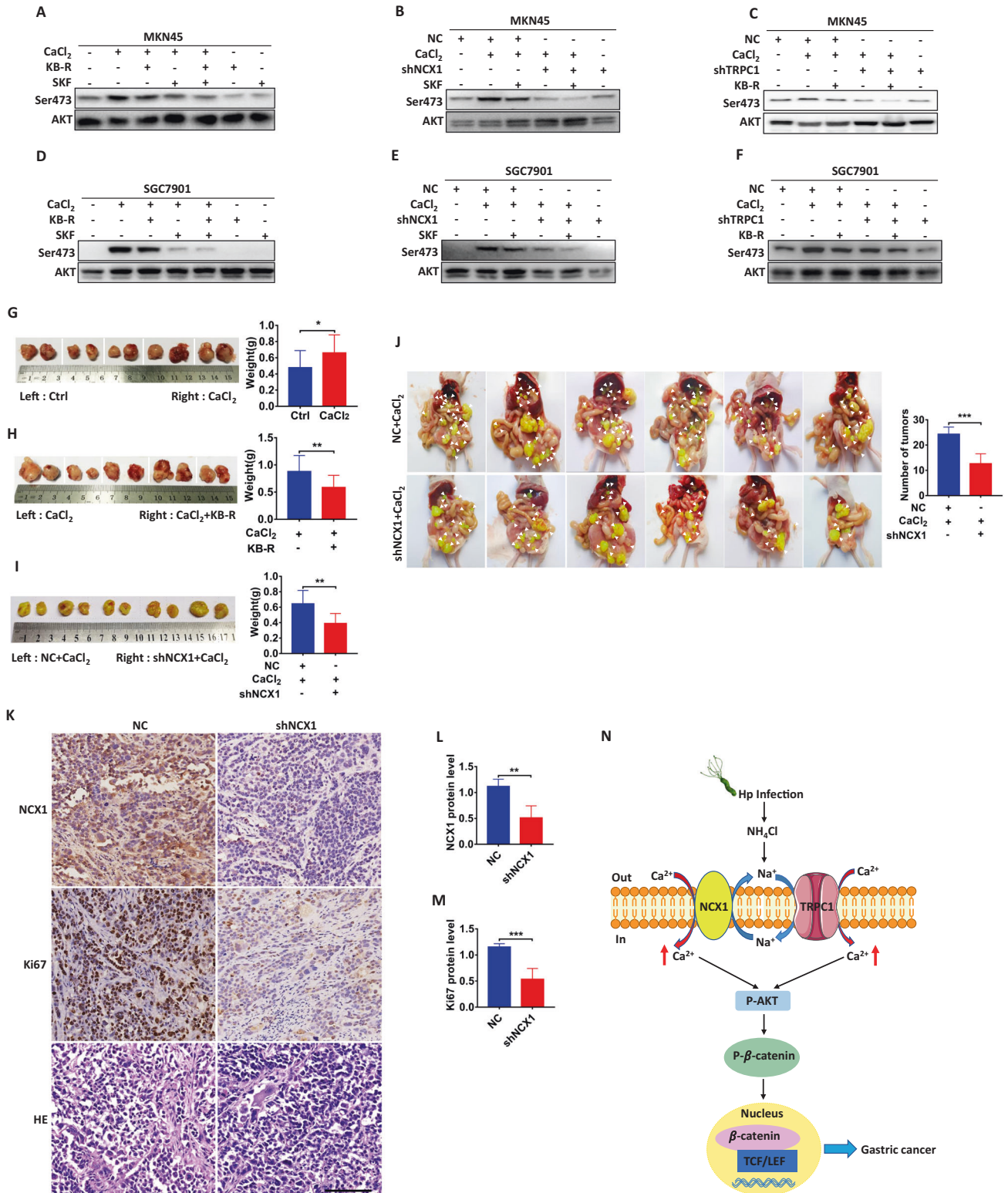


**Fig. 8** TRPC1/NCX1 coupling induces AKT phosphorylation and promotes GC growth and metastasis. **A, D** Inhibitory effects of either KB-R7943 (KB-R, 1 μM in MKN45, 8 μM in SGC7901), SKF96365 (SKF, 1 μM) or KB-R plus SKF on CaCl<sub>2</sub> (2 mM)-induced AKT phosphorylation in GC cells. **B, E** Inhibitory effects of SKF, shNCX1 or shNCX1 plus SKF on CaCl<sub>2</sub> (2 mM)-induced AKT phosphorylation in GC cells. **C, F** Inhibitory effects of either KB-R, shTRPC1 or shTRPC1 plus KB-R on CaCl<sub>2</sub>-induced AKT phosphorylation in GC cells. CaCl<sub>2</sub> promoted growth of xenografted gastric tumors (**G**), which was attenuated by either KB-R7943 (**H**) or shNCX1 (**I**). **J** Inhibitory effects of shNCX1 on CaCl<sub>2</sub>-induced gastric tumor metastasis. **K** Immunohistochemical analysis and histological examination on expression of NCX1 and Ki67 proteins with or without NCX1 knockdown in GC tissues. Scale bar = 100 μm for each image. **L, M** Summary data comparing expression of NCX1 and Ki67 proteins analyzed by immunohistochemistry between with or without NCX1 knockdown in GC tissues. (\**P* < 0.05, \*\*\**P* < 0.01, \*\*\*\**P* < 0.001, \*\*\*\**P* < 0.0001, *n* = 3; ns, no significant differences). **N** The proposed oncogenic mechanisms of TRPC1/NCX1 coupling via Ca<sup>2+</sup>/AKT/β-catenin pathway in *Hp*-associated GC.

scratch assay was performed as previously described [48]. After scratching, gently wash the cell monolayer to remove detached cells. Then, replenish with serum free medium containing different drugs. 0 and 24 h take photos respectively.

### Transwell migration and invasion assays

Transwell migration and invasion assays were performed as previously described [9]. Cells were cultured upper chamber with 200  $\mu$ L serum-free medium containing with different drugs. The lower chambers were filled with 600  $\mu$ L medium plus 10% FBS. For invasion assays, the upper surface of the polycarbonate filter was coated with 10% Matrigel (Collaborative Biomedical, USA). The cells were treated for 24 h.

### Measurement of $[Ca^{2+}]_{Cyt}$ by digital $Ca^{2+}$ imaging

$[Ca^{2+}]_{Cyt}$  imaging experiments were performed as previously described [49, 50]. The  $[Ca^{2+}]_{Cyt}$  imaging solution were described in the supplemental materials.

### Tumor xenograft and peritoneal dissemination assays in nude mice

Tumor xenograft assay was performed as previously described [11]. The male nude mice were purchased from Vital River Laboratory Animal Technology Co., Ltd (Beijing, China). Randomization and single-blinding were used for the measurement. After tumor sizes grow to 1 mm<sup>3</sup>,  $CaCl_2$  (4 mM), KB-R7943 (30  $\mu$ M), or  $CaCl_2$  plus KB-R7943 were injected into the tumors on one side of the armpits once a day, and 0.1% DMSO into the other side as controls. Similarly, the shNCX1 SGC7901 cells or negative control NC was separately injected into each side, and  $CaCl_2$  was injected into the tumors of each side once a day. Four weeks later, xenografted tumors were quantified. For the peritoneal dissemination assay,  $1 \times 10^6$  shNCX1 SGC7901 cells and the NC cells were injected into the abdominal cavity of nude mice.  $CaCl_2$  (4 mM) was injected into abdominal cavity once a day. Five weeks later, xenografted tumors were quantified.

### Statistical analysis

SPSS Statistics 26.0 (RRID:SCR\_002865, USA) and GraphPad Prism 7.0 (RRID:SCR\_002798, USA) software were used to analyze the data. All data shown are means  $\pm$  SD. All experiments were repeated for at least three times. Student's unpaired, two-tailed t test or one-way ANOVA were used to analyze statistical significance differences of experimental groups. The patient survival was examined by the log-rank test using the Kaplan-Meier method. Significant differences ( $P < 0.05$ ) are expressed in the figures and figure legends.

## REFERENCES

- Joshi SS, Badgwell BD. Current treatment and recent progress in gastric cancer. *CA Cancer J Clin*. 2021;71:264–79.
- Seo JH, Fox JG, Peek RM Jr, Hagen SJ. N-methyl D-aspartate channels link ammonia and epithelial cell death mechanisms in *Helicobacter pylori* Infection. *Gastroenterology*. 2011;141:2064–75.
- Chen J, Sitsel A, Benoy V, Sepulveda MR, Vangheluwe P. Primary Active  $Ca^{2+}$  Transport Systems in Health and Disease. *Cold Spring Harb Perspect Biol*. 2020;12:a035113.
- Patergnani S, Danese A, Bouhamida E, Aguiari G, Previati M, Pinton P, et al. Various Aspects of Calcium Signaling in the Regulation of Apoptosis, Autophagy, Cell Proliferation, and Cancer. *Int J Mol Sci*. 2020;21:8323.
- Berridge MJ. The Inositol Trisphosphate/Calcium Signaling Pathway in Health and Disease. *Physiol Rev*. 2016;96:1261–96.
- Marchi S, Giorgi C, Galluzzi L, Pinton P.  $Ca^{2+}$  Fluxes and Cancer. *Mol Cell*. 2020;78:1055–69.
- Monteith GR, Prevarskaya N, Roberts-Thomson SJ. The calcium-cancer signalling nexus. *Nat Rev Cancer*. 2017;17:367–80.
- Monteith GR, McAndrew D, Faddy HM, Roberts-Thomson SJ. Calcium and cancer: targeting  $Ca^{2+}$  transport. *Nat Rev Cancer*. 2007;7:519–30.
- Gao N, Yang F, Chen S, Wan H, Zhao X, Dong H. The role of TRPV1 ion channels in the suppression of gastric cancer development. *J Exp Clin Cancer Res*. 2020;39:206.
- Tang B, Wu J, Zhu MX, Sun X, Liu J, Xie R, et al. VPAC1 couples with TRPV4 channel to promote calcium-dependent gastric cancer progression via a novel autocrine mechanism. *Oncogene*. 2019;38:3946–61.

- Xie R, Xu J, Xiao Y, Wu J, Wan H, Tang B, et al. Calcium Promotes Human Gastric Cancer via a Novel Coupling of Calcium-Sensing Receptor and TRPV4 Channel. *Cancer Res*. 2017;77:6499–512.
- Ottolia M, Philipson KD. NCX1: mechanism of transport. *Adv Exp Med Biol*. 2013;961:49–54.
- Blaustein MP, Lederer WJ. Sodium/calcium exchange: its physiological implications. *Physiol Rev*. 1999;79:763–854.
- Chovancova B, Liskova V, Babula P, Krizanova O. Role of Sodium/Calcium Exchangers in Tumors. *Biomolecules*. 2020;10:1257.
- Rodrigues T, Estevez GNN, Tersariol I.  $Na^{+}/Ca^{2+}$  exchangers: Unexploited opportunities for cancer therapy? *Biochem Pharm*. 2019;163:357–61.
- Zhang F, Wan H, Chu F, Lu C, Chen J, Dong H. Small intestinal glucose and sodium absorption through calcium-induced calcium release and store-operated  $Ca^{2+}$  entry mechanisms. *Br J Pharm*. 2021;178:346–62.
- Kemeny LV, Schnur A, Czepon M, Rakonczay Z Jr, Gal E, Lonovics J, et al.  $Na^{+}/Ca^{2+}$  exchangers regulate the migration and proliferation of human gastric myofibroblasts. *Am J Physiol Gastrointest Liver Physiol*. 2013;305:G552–563.
- Wen J, Pang Y, Zhou T, Qi X, Zhao M, Xuan B, et al. Essential role of  $Na^{+}/Ca^{2+}$  exchanger 1 in smoking-induced growth and migration of esophageal squamous cell carcinoma. *Oncotarget*. 2016;7:63816–28.
- Xu J, Yang Y, Xie R, Liu J, Nie X, An J, et al. The NCX1/TRPC6 Complex Mediates TGFbeta-Driven Migration and Invasion of Human Hepatocellular Carcinoma Cells. *Cancer Res*. 2018;78:2564–76.
- Timmons JA, Rao JN, Turner DJ, Zou T, Liu L, Xiao L, et al. Induced expression of STIM1 sensitizes intestinal epithelial cells to apoptosis by modulating store-operated  $Ca^{2+}$  influx. *J Gastrointest Surg*. 2012;16:1397–405.
- Elzamzamy OM, Penner R, Hazlehurst LA. The Role of TRPC1 in Modulating Cancer Progression. *Cells*. 2020;9:388.
- Davis FM, Peters AA, Grice DM, Cabot PJ, Parat MO, Roberts-Thomson SJ, et al. Non-stimulated, agonist-stimulated and store-operated  $Ca^{2+}$  influx in MDA-MB-468 breast cancer cells and the effect of EGF-induced EMT on calcium entry. *PLoS One*. 2012;7:e36923.
- Dong H, Shim KN, Li JM, Estrema C, Ornelas TA, Nguyen F, et al. Molecular mechanisms underlying  $Ca^{2+}$ -mediated motility of human pancreatic duct cells. *Am J Physiol Cell Physiol*. 2010;299:C1493–1503.
- Zhang Z, Ren L, Zhao Q, Lu G, Ren M, Lu X, et al. TRPC1 exacerbate metastasis in gastric cancer via *ciRS-7/miR-135a-5p/TRPC1* axis. *Biochem Biophys Res Commun*. 2020;529:85–90.
- Ge P, Wei L, Zhang M, Hu B, Wang K, Li Y, et al. TRPC1/3/6 inhibition attenuates the TGF-beta1-induced epithelial-mesenchymal transition in gastric cancer via the Ras/Raf1/ERK signaling pathway. *Cell Biol Int*. 2018;42:975–84.
- Long Y, Wang WP, Yuan H, Ma SP, Feng N, Wang L, et al. Functional comparison of the reverse mode of  $Na^{+}/Ca^{2+}$  exchangers NCX1.1 and NCX1.5 expressed in CHO cells. *Acta Pharm Sin*. 2013;34:691–8.
- Wong JH, Ho KH, Nam S, Hsu WL, Lin CH, Chang CM, et al. Store-operated  $Ca^{2+}$  Entry Facilitates the Lipopolysaccharide-induced Cyclooxygenase-2 Expression in Gastric Cancer Cells. *Sci Rep*. 2017;7:12813.
- Li H, Xia JQ, Zhu FS, Xi ZH, Pan CY, Gu LM, et al. LPS promotes the expression of PD-L1 in gastric cancer cells through NF-kappaB activation. *J Cell Biochem*. 2018;119:9997–10004.
- Harper AG, Sage SO. TRP- $Na^{+}/Ca^{2+}$  Exchanger Coupling. *Adv Exp Med Biol*. 2016;898:67–85.
- Cai R, Ding X, Zhou K, Shi Y, Ge R, Ren G, et al. Blockade of TRPC6 channels induced G2/M phase arrest and suppressed growth in human gastric cancer cells. *Int J Cancer*. 2009;125:2281–7.
- Wang H, Deng G, Ai M, Xu Z, Mou T, Yu J, et al. Hsp90ab1 stabilizes LRP5 to promote epithelial-mesenchymal transition via activating of AKT and Wnt/beta-catenin signaling pathways in gastric cancer progression. *Oncogene*. 2019;38:1489–507.
- Zhao J, Ou B, Han D, Wang P, Zong Y, Zhu C, et al. Tumor-derived CXCL5 promotes human colorectal cancer metastasis through activation of the ERK/Elk-1/ Snail and AKT/GSK3beta/beta-catenin pathways. *Mol Cancer*. 2017;16:70.
- Fujimoto Y, Hayashi S, Azuma YT, Mukai K, Nishiyama K, Kita S, et al. Over-expression of  $Na^{+}/Ca^{2+}$  exchanger 1 display enhanced relaxation in the gastric fundus. *J Pharm Sci*. 2016;132:181–6.
- Dong H, Tang B, Jiang Y, Mittal RK.  $Na^{+}/Ca^{2+}$  exchanger 1 is a key mechanosensitive molecule of the esophageal myenteric neurons. *Acta Physiol*. 2019;225:e13223.
- Dong H, Sellers ZM, Smith A, Chow JY, Barrett KE.  $Na^{+}/Ca^{2+}$  exchange regulates  $Ca^{2+}$ -dependent mucosal ion transport and  $HCO_3^-$  secretion in mice. *Am J Physiol Gastrointest Liver Physiol*. 2005;288:G457–465.
- Tang B, Chow JY, Dong TX, Yang SM, Lu DS, Carethers JM, et al. Calcium sensing receptor suppresses human pancreatic tumorigenesis through a novel NCX1/ $Ca^{2+}$ /beta-catenin signaling pathway. *Cancer Lett*. 2016;377:44–54.



37. Mahdi SH, Cheng H, Li J, Feng R. The effect of TGF-beta-induced epithelial-mesenchymal transition on the expression of intracellular calcium-handling proteins in T47D and MCF-7 human breast cancer cells. *Arch Biochem Biophys.* 2015;583:18–26.
38. Hu HJ, Wang SS, Wang YX, Liu Y, Feng XM, Shen Y, et al. Blockade of the forward  $\text{Na}^{(+)}/\text{Ca}^{(2+)}$  exchanger suppresses the growth of glioblastoma cells through  $\text{Ca}^{(2+)}$ -mediated cell death. *Br J Pharm.* 2019;176:2691–707.
39. Liu Z, Cheng Q, Ma X, Song M. Suppressing Effect of  $\text{Na}^{(+)}/\text{Ca}^{(2+)}$  Exchanger (NCX) Inhibitors on the Growth of Melanoma Cells. *Int J Mol Sci.* 2022;23:901.
40. Wessler S, Krisch LM, Elmer DP, Aberger F. From inflammation to gastric cancer - the importance of Hedgehog/GLI signaling in Helicobacter pylori-induced chronic inflammatory and neoplastic diseases. *Cell Commun Signal.* 2017;15:15.
41. Iimuro M, Nakamura S, Arakawa T, Wakabayashi K, Mutoh M. Effects of dietary calcium on Helicobacter pylori-induced gastritis in Mongolian gerbils. *Anticancer Res.* 2013;33:3667–74.
42. Ghanayem BI, Matthews HB, Maronpot RR. Calcium channel blockers protect against ethanol- and indomethacin-induced gastric lesions in rats. *Gastroenterology.* 1987;92:106–11.
43. Tatsuta M, Iishi H, Baba M, Nakaizumi A, Uehara H, Taniguchi H. Effect of calcium channel blockers on gastric carcinogenesis and caerulein enhancement of gastric carcinogenesis induced by N-methyl-N'-nitro-N-nitrosoguanidine in Wistar rats. *Cancer Res.* 1990;50:2095–8.
44. Percie du Sert N, Hurst V, Ahluwalia A, Alam S, Avey MT, Baker M, et al. The ARRIVE guidelines 2.0: Updated guidelines for reporting animal research. *Br J Pharm.* 2020;177:3617–24.
45. Xu J, Ji B, Wen G, Yang Y, Jin H, Liu X, et al.  $\text{Na}^{+}/\text{H}^{+}$  exchanger 1,  $\text{Na}^{+}/\text{Ca}^{2+}$  exchanger 1 and calmodulin complex regulates interleukin 6-mediated cellular behavior of human hepatocellular carcinoma. *Carcinogenesis.* 2016;37:290–300.
46. Wang F, Zhang J, Tang H, Pang Y, Ke X, Peng W, et al. Nup54-induced CARM1 nuclear importation promotes gastric cancer cell proliferation and tumorigenesis through transcriptional activation and methylation of Notch2. *Oncogene.* 2022;41:246–59.
47. Takenoue T, Kitayama J, Takei Y, Umetani N, Matsuda K, Nita ME, et al. Characterization of dihydropyrimidine dehydrogenase on immunohistochemistry in colon carcinoma, and correlation between immunohistochemical score and protein level or messenger RNA expression. *Ann Oncol.* 2000;11:273–9.
48. Martinotti S, Ranzato E. Scratch Wound Healing Assay. *Methods Mol Biol.* 2020;2109:225–9.
49. Zhang F, Wan H, Yang X, He J, Lu C, Yang S, et al. Molecular mechanisms of caffeine-mediated intestinal epithelial ion transports. *Br J Pharm.* 2019;176:1700–16.
50. Wan H, Xie R, Xu J, He J, Tang B, Liu Q, et al. Anti-proliferative Effects of Nucleotides on Gastric Cancer via a Novel P2Y6/SOCE/ $\text{Ca}^{(2+)}$ /beta-catenin Pathway. *Sci Rep.* 2017;7:2459.

## ACKNOWLEDGEMENTS

These studies were supported by research grants from the National Natural Science Foundation of China (No. 81972328 to HXW, No. 81873544 to HD, and No. 82103591 to NNG).

## AUTHOR CONTRIBUTIONS

HD conceived the study, designed and supervised the experiments, wrote, revised, and finalized the manuscript. HW designed some experiments, performed most experiments and data analysis, and wrote the draft. NG performed most experiments and data analysis. WL, CL, JC and YW performed some experiments.

## COMPETING INTERESTS

The authors declare no competing interests.

## ADDITIONAL INFORMATION

**Supplementary information** The online version contains supplementary material available at <https://doi.org/10.1038/s41388-022-02412-9>.

**Correspondence** and requests for materials should be addressed to Hui Dong.

**Reprints and permission information** is available at <http://www.nature.com/reprints>

**Publisher's note** Springer Nature remains neutral with regard to jurisdictional claims in published maps and institutional affiliations.



**Open Access** This article is licensed under a Creative Commons Attribution 4.0 International License, which permits use, sharing, adaptation, distribution and reproduction in any medium or format, as long as you give appropriate credit to the original author(s) and the source, provide a link to the Creative Commons license, and indicate if changes were made. The images or other third party material in this article are included in the article's Creative Commons license, unless indicated otherwise in a credit line to the material. If material is not included in the article's Creative Commons license and your intended use is not permitted by statutory regulation or exceeds the permitted use, you will need to obtain permission directly from the copyright holder. To view a copy of this license, visit <http://creativecommons.org/licenses/by/4.0/>.

© The Author(s) 2022